On the Model of Solid State Joint Formation under Superplastic Forming Conditions

O.A. Kaibyshev, R.V. Safiullin, R.Y. Lutfullin, and V.V. Astanin

(Submitted 1 February 1996; in revised form 11 December 1998)

The peculiarities of solid state joint (SSJ) formation under conditions of superplastic forming (SPF) were investigated for the titanium alloy VT6S (Ti-6Al-4V). The influence of annealing and SPF on the change of state of the alloy surface was considered. A significant role of grain boundary sliding (GBS) in the formation of both surface microrelief and SSJ was established. It was shown that SSJ formation under SPF conditions is primarily a deformation process. Corresponding schemes of the appearance of surface microrelief and SSJ formation are proposed.

Keywords deformation, solid state joint, superplasticity, titanium alloy Ti-6Al-4V

1. Introduction

A considerable number of papers have been devoted to the nature of solid state joint (SSJ) formation (Ref 1-5). Models of SSJ formation proposed in the papers was based on compression experiments. The previously mentioned models have one common feature—the multistage character of the SSJ process, which is the formation of physical contact, its activation, and volume interaction. The development of recrystallization resulting in the formation of common grains in the contact area is considered to be the criterion for the completion of the solid state bonding process (Ref 2). In these cases the role of deformation, including the superplastic role (Ref 2, 3), comes down only to the accelerated formation of physical contact due to plastic collapse of surface asperities, that is, local deformation in the joint area. An analogous approach is used in this article (Ref 6) to describe the SSJ process under conditions of superplastic forming. The conditions of SSJ formation in real constructions obtained by superplastic forming/diffusion bonding (SPF/DB) technology differ considerably from the conditions discussed previously.

Sheet materials, which are used for production of multilayer structures, are subjected to significant tensile deformation. In some cases this deformation occurs prior to the joining process, while in other cases it occurs after the joint is formed. The latter case was considered by Kaibyshev, Lutfullin, and Berdin (Ref 7, 8) in which the improvement of SSJ quality after superplastic (SP) deformation and the absence of recrystallization in the joint area were established experimentally. But the influence of prior superplastic forming (SPF) on the SSJ formation remained unclear until now.

The role of SP deformation before diffusion bonding can be examined from two viewpoints: (a) the change of the microrelief on the surface of the formed sheet relative to the initial polished surface and (b) the change of the microstructure in the vicinity of the bonded interface. There is an opinion that the surface roughness (microrelief) negatively affects the SSJ process. The time necessary for establishing complete physical contact between surfaces and the porosity in the joint area are increased (Ref 9). Reference 10 provides data concerning the increase of the surface roughness at SP deformation, and it is proposed that roughness can negatively influence the mechanical properties of the bonded joint as well. However, no experimental evidence for this idea is given.

Beck and Knepper (Ref 11) connect the increase of the surface roughness with grain boundary sliding (GBS)—the main mechanism of superplastic deformation. Meanwhile, GBS and its role in SP deformation are intensively being studied presently. New data on mesoscopic localization at SP deformation in the form of "cooperative" GBS have recently been published (Ref 12-15). The goal of the present work is to reveal the influence of SP deformation on kinetics and the mechanism of SSJ formation in the titanium sheet alloy Ti-6Al-4V during the SPF/DB process.

2. Experimental Procedures

The ($\alpha + \beta$) titanium alloy VT6S (Ti-6Al-4V) in the form of sheets 0.6 mm thick with structural superplasticity was the object of the investigation. In the initial state it had a microcrystalline structure with a grain size within 1 to 3 μm.

The effect of heating on the structure and the state of the sheet surface were determined by annealing the alloy specimens with initially polished surfaces (R_a = 0.02 μm) in an argon atmosphere at 900 °C in accordance with the temperature regime where SP operations were performed on this alloy (Ref 16). The samples were water cooled. Annealing time varied from 15 min to 6 h. Superplastic forming of polished sheet specimens was carried out according to the scheme given in Fig. 1. The specimens were sealed into an airtight container and put into tooling with a replaceable matrix (die). The diameter of the cylindrical hole in the matrix, *d*, was 30 mm. The depth of forming, *h*, was 5, 10, and 15 mm for obtaining different deformation degrees. Because in each point of the forming dome

O.A. Kaibyshev, R.V. Safiullin, R.Y. Lutfullin, and **V.V. Astanin,** Institute for Metals Superplasticity Problems, Russian Academy of Science, Khalturina 39, Ufa, 450001, Russia.

two-axis extension occurred, the method described in detail in Ref 17 was used for quantitative evaluation of the deformation degree. According to this method, the value of the accumulated strain for an arbitrary point (between pole and edge) of the dome being formed can be calculated from the measured values of the initial specimen (sheet) thickness, S_0, and resulting thickness, S, in accordance with the following estimation:

$$e = (1.000 \ldots 1.155) \ln (S_0/S) \quad \text{(Eq 1)}$$

For convenience of comparison of the data obtained with available experiments on uniaxial tensile tests, the concept of equivalent strain can be used:

$$\varepsilon_{eq} = [\exp(e) - 1]\ 100\% \quad \text{(Eq 2)}$$

where the value of accumulated strain, e, can be estimated on the basis of Eq 1.

Superplastic forming of specimens was conducted at temperature, T, of 900 ± 5 °C. Strain rate, $\dot{\varepsilon}$, was $5 \times 10^{-4} s^{-1}$, which corresponds to the optimal value for the given alloy (Ref 16). The equivalent tensile strain varied from 20 to 400%.

Specimens for microstructural investigations were cut using the electric-discharge method from the bottom portion of formed domes. The surface roughness was measured by means of a profilograph-roughness indicator ME-10 on five basic lengths. The value of an average-arithmetic profile deviation, R_a, expressed in micrometers was used as the main parameter characterizing the microrelief height. Microstructural investigations were carried out using an electron microscope (JSM-840; JEOL, Japan) over three cross sections with magnification from 5 to 2000×. The investigation of SPF influence on SSJ formation was conducted by the same method using the counterforming of two polished specimens. After a definite forming time, the sheet specimens were separated, and the surfaces in mutual contact were studied.

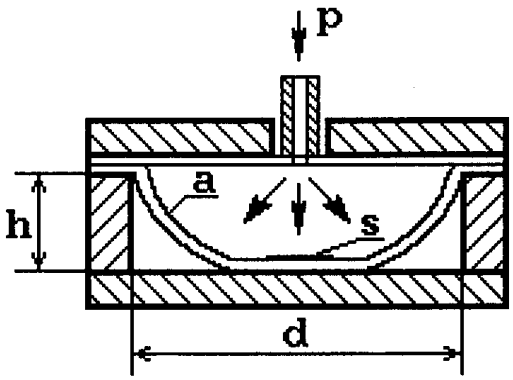

Fig. 1 The scheme of an SPF experiment: a, sheet being formed; p, argon pressure; s, zone for deformation relief investigation

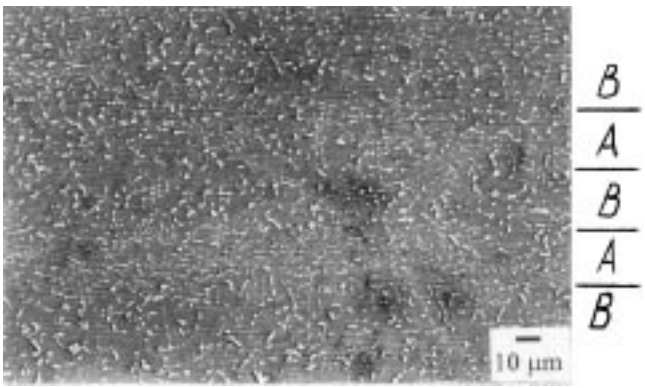

(a)

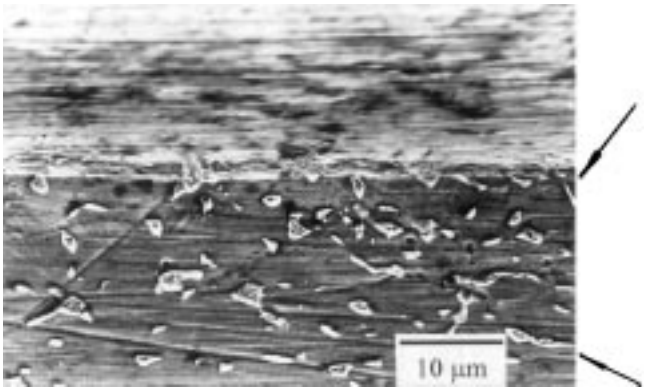

(b)

Fig. 2 The initial structure of VT6S alloy. (a) The cross section of the sheet shows A bands containing aligned contiguous α- and β-phase grains between which there are B bands containing nonaligned, uniformly distributed α- and β-phase grains. (b) In the B zone, arrows show α-phase chains tilted to the surface at an angle of about 45°.

3. Results and Discussion

3.1 Sheet Structure

The initial structure at the sheet cross section (Fig. 2a) was nonuniform, which is typical of such alloys (Ref 18). The micrograph shows an A band containing aligned contiguous α and β, the phase grains between which there is a B band containing nonaligned, uniformly distributed α- and β-phase grains. This is a result of the metallurgical process including rolling. Region B shows aligned chains oriented at an angle of nearly 45° to the sheet surface (Fig. 2b). This peculiarity is evidently also a result of rolling.

The annealing, equivalent to heating before forming, resulted in the formation of a microduplex structure with the phase relation α:β = 60:40 and mean grain sizes of the α-phase, 3.5 μm, and of the β-phase, 3.4 μm. During annealing in the argon atmosphere, the sublimation of atoms from the surface of specimens led to the occurrence of grooves in the grain boundaries, and etch patterns in the α-phase appeared. Meanwhile during 2.2 h (time equivalent to deformation up to 400%), the roughness quantity insignificantly increased and varied from 0.02 to 0.04 μm.

The investigation of specimens subjected to SPF made it possible to establish that deformation along different directions

occurs nonuniformly. The deformation across rolling direction was on the average 5% higher than that in the longitudinal direction, which was explained by inhomogeneity of the initial structure (Ref 18). It has been noted that in A band areas, deformation was often absent, even when total sheet deformation reached $\varepsilon_{eq} = 20\%$.

3.2 Deformation Relief

Deformation led to the appearence of a typical wavy relief on the surface. The long bands align in the rolling direction (Fig. 3). The wave height varies from 6 to 8 μm at $\varepsilon = 25\%$ to 50 to 60 μm at $\varepsilon = 400\%$. The distance between waves ranges between 1 and 3 mm. The macrorelief observed in this case had the form of either bands ($\varepsilon < 100\%$) or cells ($\varepsilon > 100\%$).

At greater magnification (Fig. 4a), the relief formed by GBS is seen, and marker lines displacement and vertical steps along grain boundaries are observed. Sliding is not uniform, but in the form of localized deformation bands (LDBs), it is characterized by specific bright contrast. The LDBs are preferably situated in regions containing nonaligned uniformly distributed α- and β-phase grains, that is, in B regions, and are mainly orientated either in the direction of rolling or at an angle of 45° to this direction. They seem to frame the fragments of several α-phase grains. Inside these fragments a less intensive shift of separate grains is observed. At deformation up to 40%, the number of LDBs in A regions is minimum or they are absent. At increasing ε, LDBs begin to develop, but less intensively than in B regions.

Figure 4(b) shows that aligned chains of β-phase inside of the sheet correspond to the bands of intensive deformation on the surface. This fact supports the view suggested in Ref 18 concerning the dominant sliding along α-β and β-β boundaries. Moreover, the analysis of Fig. 4(a) and (b) indicates the action of "cooperative" GBS, which was schematically predicted in Ref 18 but not revealed experimentally.

As the strain degree increased, the number of deformation bands considerably rose as a consequence of their development inside the fragments, which led to intensive dividing of the latter. As a result, at strains more than 100%, separate deformation bands cannot be practically distinguished. Further increase of strain up to 400% led to observation of separate grains on the surface. Figure 5 shows the change of surface roughness at increasing ε. The comparison of the values of surface roughness in the VT6S alloy after annealing and SPF demonstrates that at the similar time parameters (duration of annealing and that of SP deformation), the value R_a after SPF is larger than that in annealed sheet samples by more than an order of magnitude. This allows the neglect of sublimation relief hereinafter.

The development of the deformation process and the formation of the surface relief during forming of the given alloy can be explained using the concept of "cooperative" GBS for two-phase alloys Zn-22%Al (Ref 12, 15), lead-tin eutectic (Ref 16), and intermetallic Ti_3Al (Ref 13). The nucleation of a band of "cooperative" GBS is most likely to occur in the areas where the boundaries of sequential grains are aligned one after another along the direction of maximum tangential stresses or close to this direction (Fig. 6a). Plane angles between such boundaries must approximate 180 °C (Ref 15). The second

Fig. 3 The sheet surface macrorelief connected with the nonuniformity of structure, $\varepsilon_{eq} = 40\%$. The rolling direction is horizontal.

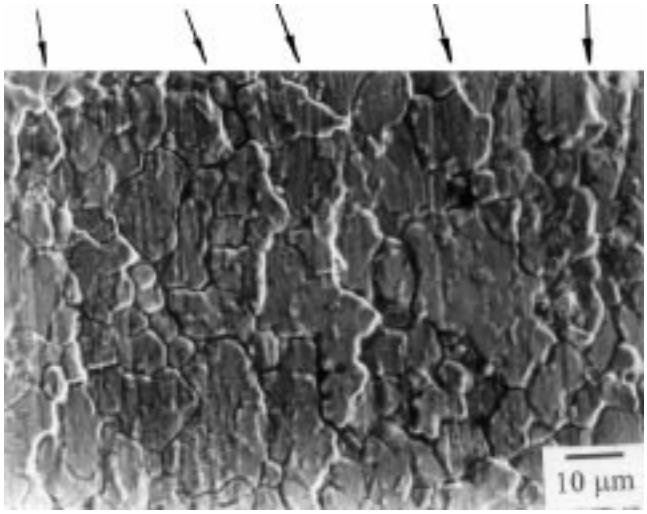

(a)

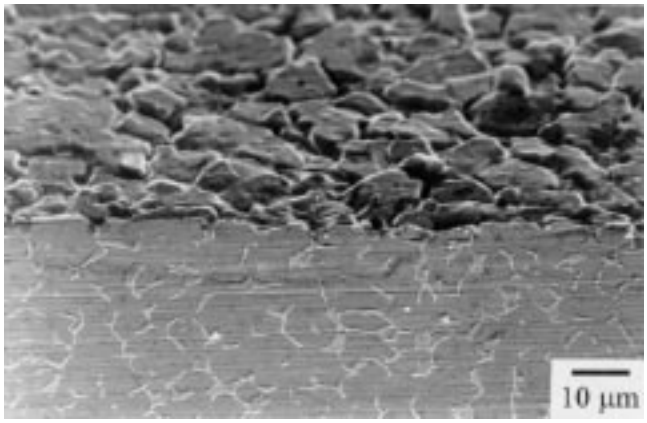

(b)

Fig. 4 The deformation microrelief of the (a) sheet surface and the (b) microstructure of the cross section. Arrows show localized deformation bands, $\varepsilon = 20\%$. The rolling direction is vertical.

condition may be that these boundaries have minimum resistance to sliding. In the case of the given alloy, the boundaries of α-β or β-β type meet this condition (Ref 18). In the initial structure of the alloy, there were elongated β-phase particles forming chains of different length mainly along boundaries of α-grains fragments (Fig. 2b), and their number increased due to SP deformation (Fig. 4b). The latter fact testifies to the existence of the effect of self organization of "cooperative" GBS development by a mechanism that is not clear at present.

"Cooperative" GBS bands that were originally several grain sizes long gradually spread in the sheet interior and came to the surface to form relatively large steps (Fig. 6b), which explains the roughness increase. An increase of the strain degree resulted in the appearance of new directions favorable for GBS. Due to the development of deformation bands, the division of large fragments of the α-phase and the decrease of grain group sizes occurred (Fig. 6c). At considerable strains due to the increase of band number, the distance between them decreased to the size of individual grains, which were visible on the surface of deformed sheets (Fig. 6d).

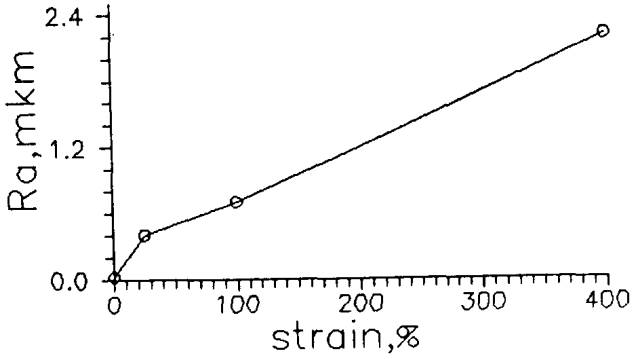

Fig. 5 The change of the surface roughness, R_a, depending on a strain

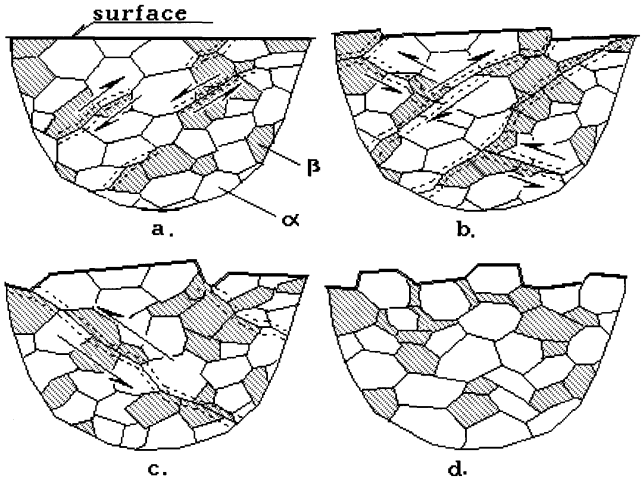

Fig. 6 The scheme of formation of deformation relief. (a) Nucleation of localized deformation bands. (b) Coming out of developed bands to the surface and nucleation of new bands. (c) Formation of grain fragments. (d) Division of relief into separate grains at high strains

3.3 Solid State Joint Formation

The process of two-sheet joint formation at SPF and solid state bonding began along bulges that resulted from localized deformation. Figure 7(a) shows traces of ductile fracture on the surface of specimens separated after initial bonding. The character of these traces coincides with the configuration of deformation bands observed on the surface of a formed specimen (Fig. 4a). It should be noted that in the zones where the bands of "cooperative" GBS came to the surface, the instantaneous tearing of sheets with formation of a sound metallic bond is likely to occur.

After generation of primary points of tearing, the character of sheet deformation changed, which is demonstrated by deformation relief (Fig. 7b). Grain boundary sliding became more uniform, individual grains were separated by deep grooves, and open pores were revealed. The marked grains were in contact with the surface of the opposite sheet (prints were noticeable), but no sound metallic bond appeared in these zones. Brittle intercrystalline rupture prevailed.

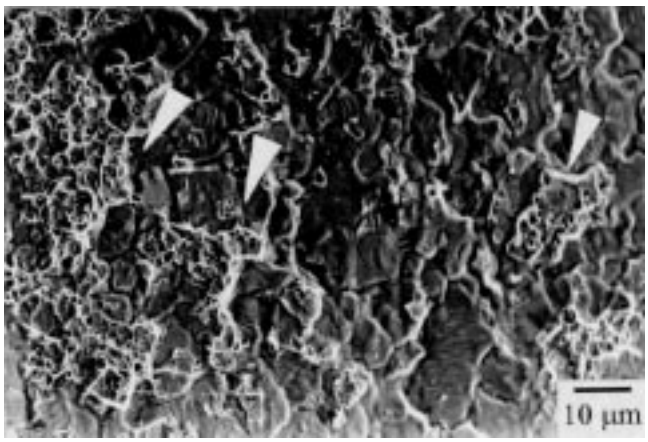

(a)

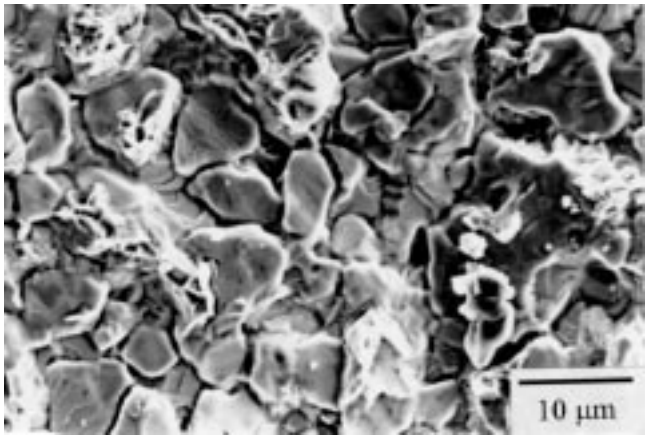

(b)

Fig. 7 The fracture surfaces of joined sheets after (a) 14% and (b) 20% equivalent deformation. Arrows show the points of primary joining in LDBs. Typical grains, which were concerned with the surface of the other sheet through an interface, are marked by "A".

The final bonding was obtained due to further forming after surface contact. Figure 8 shows characteristic features: chains of β-phase often cross the line of the bonded joint and form displacements in it. This shows that GBS not only occurred in the final stage of SSJ, but that a combined cooperative GBS of grains of different sheets also occurred. The role of β-phase in pore "healing" is also shown. More plastic β-phase penetrated into long pores dividing them into smaller pores; during further deformation it filled pores.

The strain value before the contact of surfaces exerted a certain effect on the bonding process. Strain increasing led to large grain groups dividing into smaller groups (up to individual grains), and the area of primary bonding increased. So the surface roughness increased in this case. It resulted in greater bending of the final bonding interface. On the whole, both factors added to the strength of the bonded joint (Table 1).

The analysis of experimental results obtained by means of SPF/DB technology made it possible to understand the sequence of SSJ formation under SPF conditions (Fig. 9). The proposed scheme, unlike the scheme described in Ref 6, consists of only three stages with a different physical essence at each stage.

In stage I, point contacts in the bonded surfaces were formed over peaks of deformation relief. It is important to emphasize that point contacts appeared in the α-phase zones bulging out due to action of LDBs. This determined the characteristic distance between points of setting and the peculiarity of further deformation of sheets. Unusually rapid interaction in these zones was due to the high activating ability of cooperated GBS. This can be explained by a local increase of heat energy in the areas where bands came to the sheet surface, but the accelerated cleaning (uvenilization) of the previously mentioned surface areas, as a result of high diffusion activity in LDBs, seems to be more probable. Both suppositions are indirectly supported by appearance of sublimation grooves during deformation of the given alloy (Fig. 4) and the magnesium alloy (Ref 14), as well as by abnormal growth of β-crystals on the specimen surface at SP deformation of the Zn-22%Al alloy (Ref 15).

In stage II, the character of deformation of sheets changed considerably. Because the sheets were already connected by points at a distance of several grains from each other, the deformation localization by means of "cooperative" GBS rough bands became impossible. Sliding occurred more uniformly along boundaries of separate grains, which meant a sharp reduction of the intensity of this process and, consequently, of its activating effect on SSJ. Stage II resulted in the increase of the contact area of 80 to 90%, but some interface between sheets still existed, with this interface weakening the bonded joint. The latter was demonstrated by the character of joint failure (Fig. 7b). The nature of this interface is not clear in many respects. It can be associated with gas adsorption and with other impurities that have not had time to dissolve in titanium.

In stage III, the combined deformation of connected sheets was completed, complete physical contact was established, and the interface disappeared. This occurred due to the common action of several processes: combined GBS and rotation of grains in contact, penetration of β-phase along interface and into pores, diffusion dissolution of adsorbed impurities, and pore "healing." In this stage the role of diffusion, including volume one, became dominant, while at previous stages diffusion was mainly an accommodational process. Contrary to the widespread opinion, the data available did not show any prominent role of recrystallization in the last stage of SSJ formation. Probably, it was specific for the given two-phase alloy. Thus, the deformational process and, in particular, "cooperative"

Table 1 Results of SPF deformation

Forming depth (Fig. 1), *h*,mm	0	5	10
Deformation for the pole, εp, %	0	20	108
Deformation for the edge,ε_e, %	0	53	270
Average bottom deformation, $\varepsilon_{avg} = (2\varepsilon_e + \varepsilon_p)/3$, %	0	42	214
Tearing gas pressure, P_t, MPa	1	1.5	2.2
Tearing force, F_t, kN	0.95	1.97	2.89
Area of tearing, %	…	69.5	87

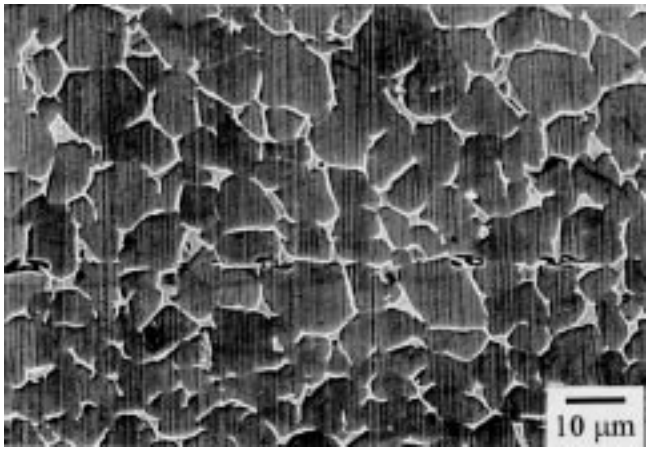

Fig. 8 The structure of a bonded joint in the final stage ε_{eq} = 34%. The joint plane is horizontal.

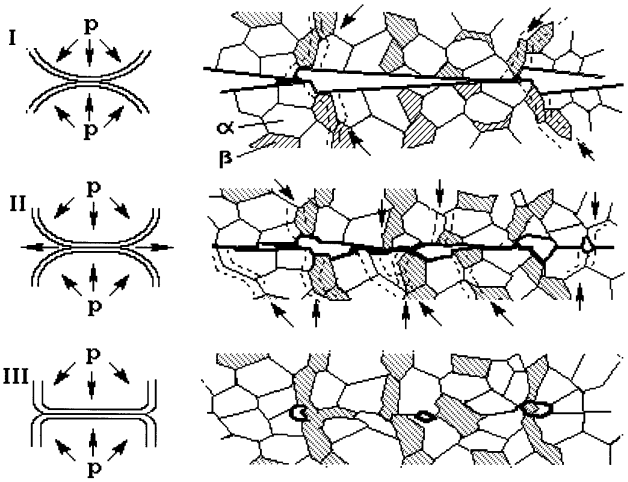

Fig. 9 The scheme of SSJ formation at SPF. (a) Stage I: initial tearing in the areas of coming out of "cooperative" GBS bands to the surface. (b) Stage II: formation of joint with separation surface due to deformation of regions between tearing points. (c) Stage III: deformation-diffusional elimination of separation surface and pore "healing"

GBS play an important role in all the stages of SSJ formation during SPF. They provide physical contact, clearing, and activation of surfaces being connected, which considerably reduces the time of SSJ formation. At the same time, it should be admitted that further investigation is necessary for a more complete understanding of the nature and mechanisms of SSJ formation at SPF.

4. Conclusions

The following conclusions have been drawn from this investigation:

- Under SPF conditions, a wavy macrorelief appears on the surface of titanium alloy VT6S (Ti-6Al-4V) sheets. Alongside macrorelief, the microrelief formed under SPF conditions. With increasing strain degree the surface roughness increased from 0.02 μm in the initial state to 2.2 μm at ε = 400%.
- Localized deformation in the form of "cooperative" GBS bands, which mostly spread along α/β interfaces, was the main contribution to the formation and development of microrelief. Increasing the strain increased the number of bands.
- A new process for the development of surface relief during SPF and a process for formation of a solid state joint under SPF/DB conditions are suggested.

References

1. Y.L. Krasulin, *Solid-Phase Interaction of a Metal with a Conductor*, Nauka, 1971 (in Russian)
2. E.S. Karakozov, *Pressure Welding of Metals*, Mashinostroenie, 1986 (in Russian)
3. M.K. Shorshorov, E.M. Dzneladze, A.S. Tihonov, E.S. Karakozov, and B.A. Matushkin, Solid State Bonding of OT4, VT6 and VT15 Titanium Alloys under Superplastic Conditions, *Weld. Prod.*, No. 10, 1975, p 20-22 (in Russian)
4. R.A. Musin, V.N. Ansiferov, and V.F. Kvasniski, Diffusing Bonding of the Superalloys, *Metallurgia*, Moscow, 1979 (in Russian)
5. P.G. Partridge and C.H. Ward-Close, Application of Diffusion Bonding to Advanced Materials, *Adv. Mater. Technol. Int.*, London, 1990, p 250-256
6. P.J. Winkler, Diffusion Bonding and Superplastic Forming, Two Complementary Manufacturing Techniques, *Superplasticity and Superplastic Forming*, C.H. Hamilton and N.E. Paton, Ed., The Minerals, Metals and Materials Society, 1988, p 491-506
7. O.A. Kaibyshev, R.Y. Lutfullin, and V.K. Berdin, The Mechanism of Solid Phase Joint Formation under Superplastic Condition, *Dokl. Akad. Nauk*, Vol 319 (No. 3), 1991, p 615-618 (in Russian)
8. O.A. Kaibyshev, R.Y. Lutfullin, and V.K. Berdin, The Effect of Superplasticity on the Solid State Weldability of the Titanium Alloy Ti-4.5Al-3Mo-1V, *Acta Metall.*, Vol 42 (No. 8), 1994, p 2609-2615
9. P.G. Partridge, Superplasticity, *AGARD Lecture Series—Diffusion Bonding of Metals*, Vol 5 (No. 154), 1987, p 1-29
10. P.G. Partridge and D.V. Dunford, *Superplasticity and Superplastic Forming*, C.H. Hamilton and N.E. Paton, Ed., The Minerals, Metals and Materials Society, 1988, p 215-220
11. W. Beck and P. Knepper, *Proc. 2nd Intern. Conf. on Welding and Brazing in Aircraft and Spacecraft Construction*, German Welding Institute, Essen, 1985, p 63
12. V.V. Astanin, O.A. Kaibyshev, and S.N. Faizova, Cooperative Grain Boundary Sliding under Superplastic Flow, *Scr. Metall.*, Vol 25 (No. 12), 1991, p 2663-2668
13. H.S. Yang, M.G. Zelin, R.Z. Valiev, and A.K. Mukherjee, Strain Induced Morphological Changes of α_2 and β Phases in Ti_3Al Alloys during Superplastic Deformation, *Scr. Metall.*, Vol 26, 1992, p 1702-1712
14. M.G. Zelin, N.A. Krasilnikov, R.Z.Valiev, M.W. Grabski, H.S. Yang, and A.K. Mukherjee, On the Microstructural Aspects of the Nonhomogeneity of Superplastic Deformation at the Level of Grain Groups, *Acta Metall.*, Vol 42 (No. 1), 1993, p 119-126
15. V.V. Astanin, O.A. Kaibyshev, and S.N. Faizova, The Role of Deformation Localization in Superplastic Flow, *Acta Metall.*, Vol 42 (No. 8), 1994, p 2617-2622
16. O.A. Kaibyshev, Superplasticity of Alloys, *Intermetallics and Ceramics*, Springer-Verlag, 1992
17. R.V. Safiullin and F.U. Enikeev, Superplasticity and Superplastic Forming, A.K. Ghosh and T.R. Bieler, Ed., The Minerals, Metals and Materials Society, 1995, p 213-217
18. P.G. Partridge, D.S. McDarmaid, and A.W. Bowen, A Deformation Model for Anisotropic Superplasticity in Two Phase Alloys, *Acta Metall.*, Vol 33 (No. 4), 1985, p 571-577